

Measured Energy Transport in the MST Reversed-Field Pinch

T.M. Biewer, J.K. Anderson, B.E. Chapman, S.D. Terry¹, J.C. Reardon, N.E. Lanier²,
G.Fiksel, D.J. Den Hartog, S.C. Prager, and C.B. Forest

University of Wisconsin-Madison

¹*University of California-Los Angeles*

²*Los Alamos National Lab*

Profile measurements in standard and improved confinement (Pulsed Poloidal Current Drive) plasmas have been made in the MST using recently installed or upgraded diagnostics. Estimates of electron thermal diffusivities based upon a diagonal transport relationship indicate a 5 fold reduction in core transport during PPCD. New profile information has been obtained from the following diagnostics: T_e from Thomson scattering, majority T_i from Rutherford scattering, n_e and n_H from coupled FIR interferometry and D_α arrays. Using equilibrium reconstructions, profiles are mapped onto magnetic flux coordinates, and thermodynamic fluxes (Γ , \mathbf{q}) and forces (∇n , ∇T) are estimated for energy and particle transport. Profile measurements are compared with theoretical models based on magnetic field stochasticity (such as those of Rechester-Rosenbluth and Harvey.)

This work was supported by the U.S. D.O.E.

Motivation

- Ongoing improvements to the diagnostic arsenal of the Madison Symmetric Torus have initiated new investigations into the plasma physics of MST transport.
- The use of Pulsed Poloidal Current Drive (PPCD) in the past has demonstrated improved confinement in the MST, based on central electron temperature measurements and a hypothesized profile shape.
- Recent upgrades of the Thomson scattering system have facilitated measurements of the T_e profile in the MST out to $r/a=0.88$.
- These measurements, when coupled with density profiles from FIR Interferometry and MSTFIT reconstructed equilibria, have made it possible to calculate many transport quantities, including the electron thermal conductivity χ_e .
- If the conductivity is assumed to behave as predicted by Rechester-Rosenbluth theory, then it is possible to make a direct comparison between the expected magnetic fluctuation profile and one calculated from the linear eigenfunction code, RESTER.

Outline

- Abstract
- Motivation
- Transport Equations
- Measured T_e and n_e Profiles
- MSTFIT Reconstructed Equilibrium Quantities
- Particle Flux and Radial Electric Field Calculations
- Heat Flux and Thermal Conductivity
- Magnetic Fluctuation Level Implications
- Conclusions

Transport Equations

- Including possible sources and sinks of energy and particles, the equations of continuity and energy balance with a radial, ambipolar electric field are:

$$\frac{\partial n}{\partial t} = -\frac{1}{r} \frac{\partial}{\partial r} (r\Gamma) + S_p \qquad \frac{\partial}{\partial t} \left(\frac{3}{2} nT \right) = qE_a \Gamma - \frac{1}{r} \frac{\partial}{\partial r} (rQ) + S_E$$

- Solving for the particle and heat fluxes:

$$\Gamma_e = \frac{1}{r} \int r \left(S_{p,e} - \frac{\partial n_e}{\partial t} \right) \partial r$$

$$Q = \frac{1}{r} \int r \left(S_E + qE_a \Gamma - \frac{\partial}{\partial t} \left(\frac{3}{2} nT \right) \right) \partial r$$

- For electrons in a 3 component plasma (e^- , p^+ , impurity Z), we can write:

$$S_{p,e} = n_e n_H \langle \sigma_i v \rangle$$

$$S_{E,e} = P_e - P_{ei} - P_{ez} - P_{rad}$$

$$P_e = \eta j^2$$

$$P_{ei} = \frac{m_e}{m_i} n_i n_e e^4 \frac{\ln(\Lambda)}{4\epsilon_0} (T_e - T_i) \sqrt{2/\pi^3 m_e T_e^3}$$

$$P_{ez} = \frac{m_e}{m_z} n_z n_e Z^2 e^4 \frac{\ln(\Lambda)}{4\epsilon_0} (T_e - T_z) \sqrt{2/\pi^3 m_e T_e^3}$$

$$P_{rad} = C_{rad} (r/a)^8 P_e$$

- Thus, an expression for E_a would enable us to determine both particle and heat fluxes from measurable quantities.

Transport Equations (continued 1)

- The kinetically derived Fokker-Plank Equation for a plasma, including an ambipolar, radial electric field is:

$$\left(\frac{\partial f}{\partial t}\right)_m = \frac{|v_{\text{par}}|}{r} \left(\frac{\partial(rD_m)}{\partial r} + \frac{qE_a}{mv_{\text{par}}} \frac{\partial(rD_m)}{\partial v_{\text{par}}} \right) \left(\frac{\partial f}{\partial r} + \frac{qE_a}{mv_{\text{par}}} \frac{\partial f}{\partial v_{\text{par}}} \right)$$

- Taking the first two moments of this equation and comparing to the source free continuity ($\frac{\partial n}{\partial t} = -\frac{1}{r} \frac{\partial}{\partial r}(r\Gamma)$) and energy balance ($\frac{\partial}{\partial t}(\frac{3}{2}nT) = qE_a\Gamma - \frac{1}{r} \frac{\partial}{\partial r}(rQ)$) equations leads again to expressions for the particle and heat flux:

$$\Gamma = -Dn \left(\frac{1}{n} \frac{\partial n}{\partial r} + \frac{1}{2T} \frac{\partial T}{\partial r} - \frac{qE_a}{T} \right)$$

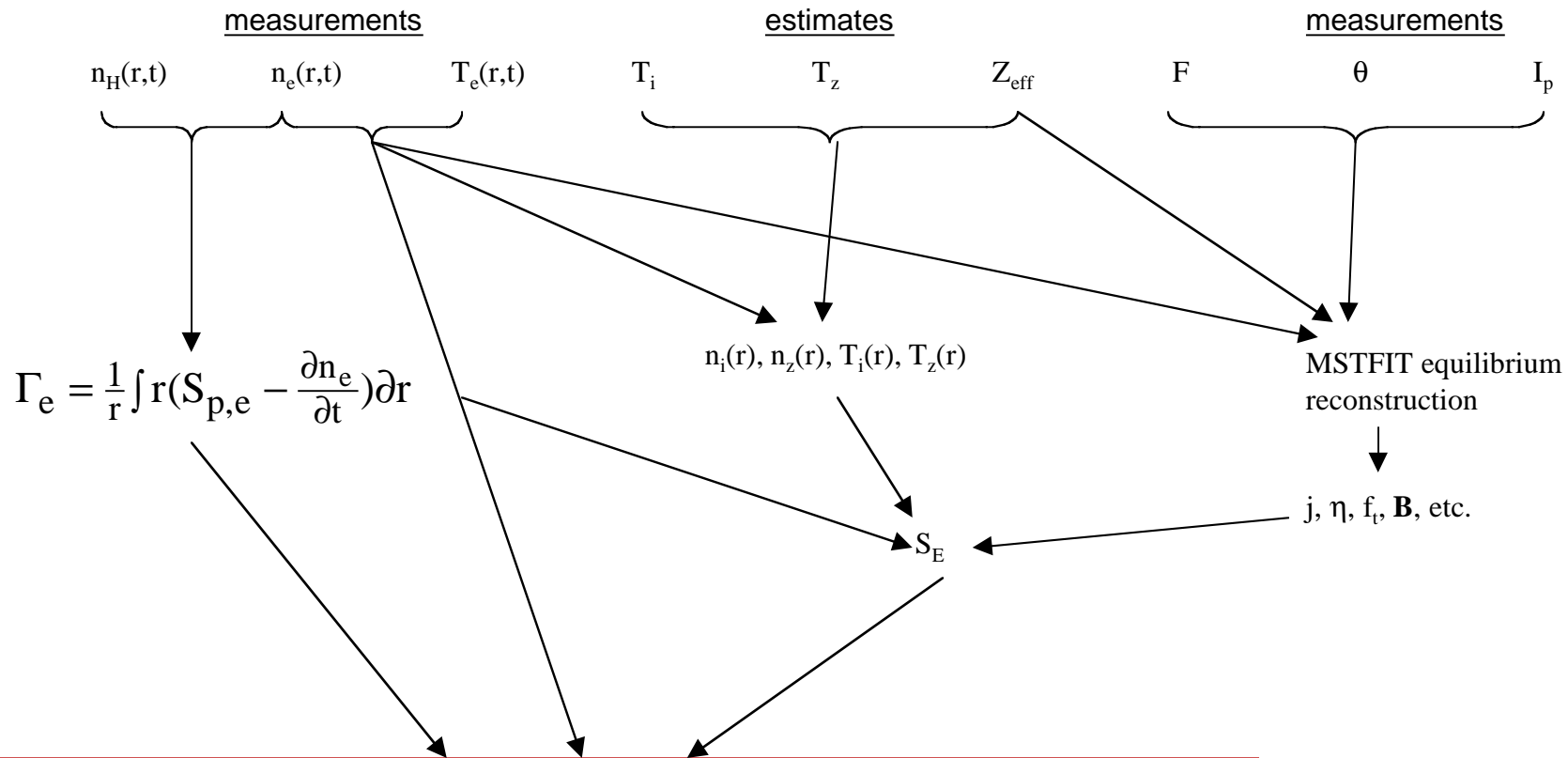
$$Q = -2DnT \left(\frac{1}{n} \frac{\partial n}{\partial r} + \frac{3}{2} \frac{1}{T} \frac{\partial T}{\partial r} - \frac{qE_a}{T} \right)$$

- By making the identification ($\chi = \frac{2}{\sqrt{\pi}} v_{tD_m} = 2D$), these expressions can be combined to yield a relation for the convective and conductive parts of the heat flux:

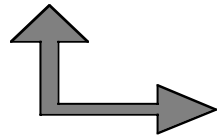
$$Q = 2\Gamma T - \chi n \frac{\partial T}{\partial r} = Q^{\text{conv}} + Q^{\text{cond}}$$

- This process introduces two new equations, but only one additional, unknown quantity (the thermal conductivity), allowing us to solve the system and determine all the quantities of interest.

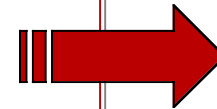
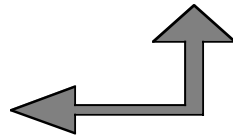
Transport Equations (continued 2)



$$\Gamma = -\frac{\chi}{2} n \left(\frac{1}{n} \frac{\partial n}{\partial r} + \frac{1}{2T} \frac{\partial T}{\partial r} - \frac{qE_a}{T} \right) \longleftrightarrow Q = \frac{1}{r} \int r \left(S_E + qE_a \Gamma - \frac{\partial}{\partial t} \left(\frac{3}{2} nT \right) \right) \partial r$$

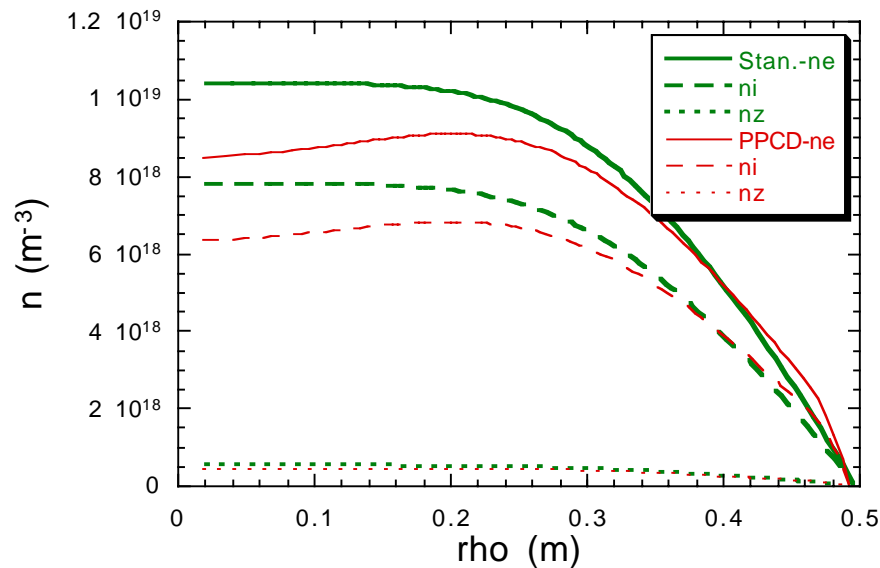
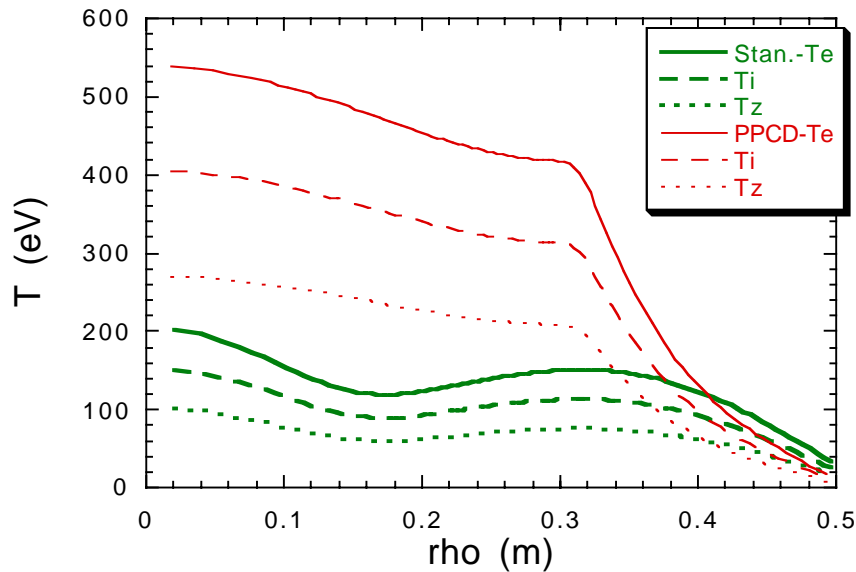


$$Q = 2\Gamma T - \chi n \frac{\partial T}{\partial r}$$



$$Q_e, \Gamma_e, \chi_e, E_a$$

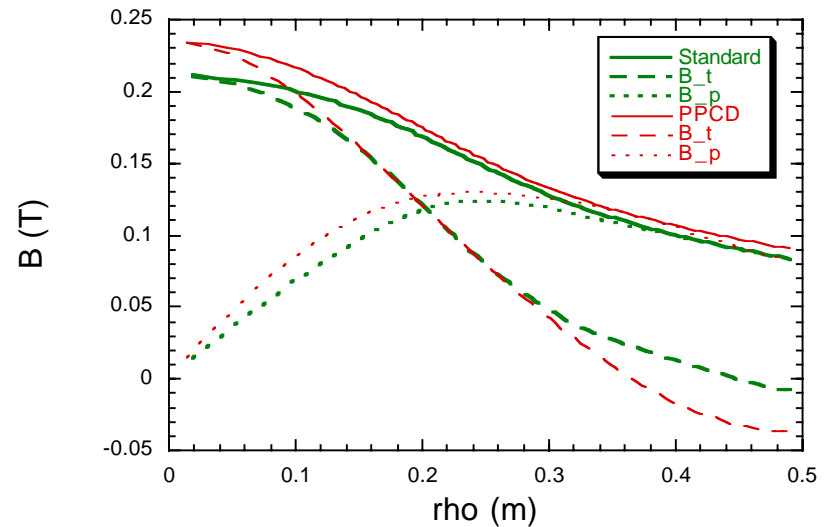
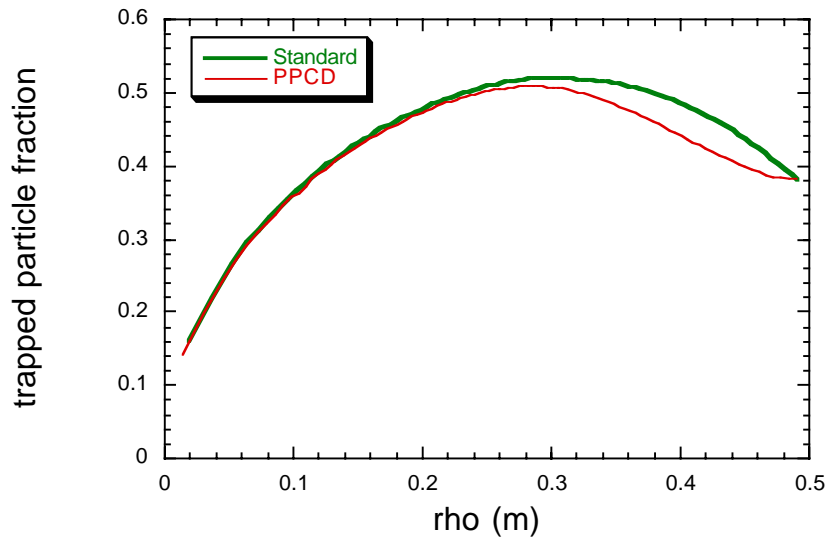
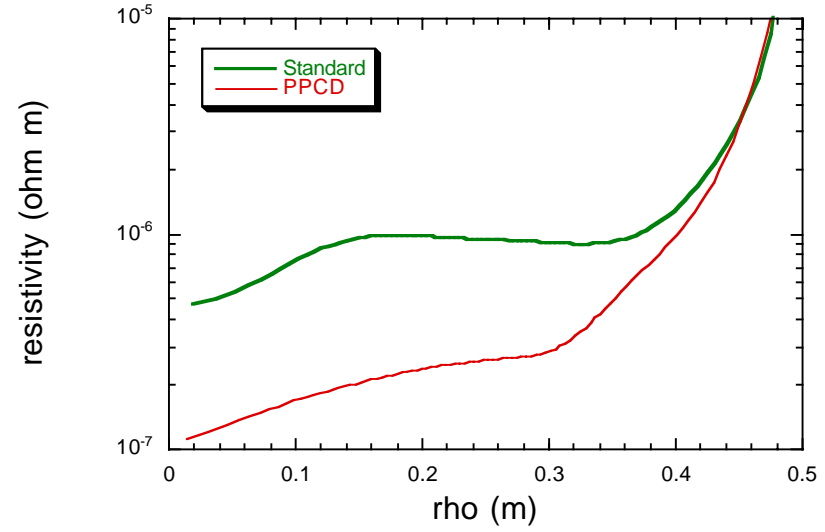
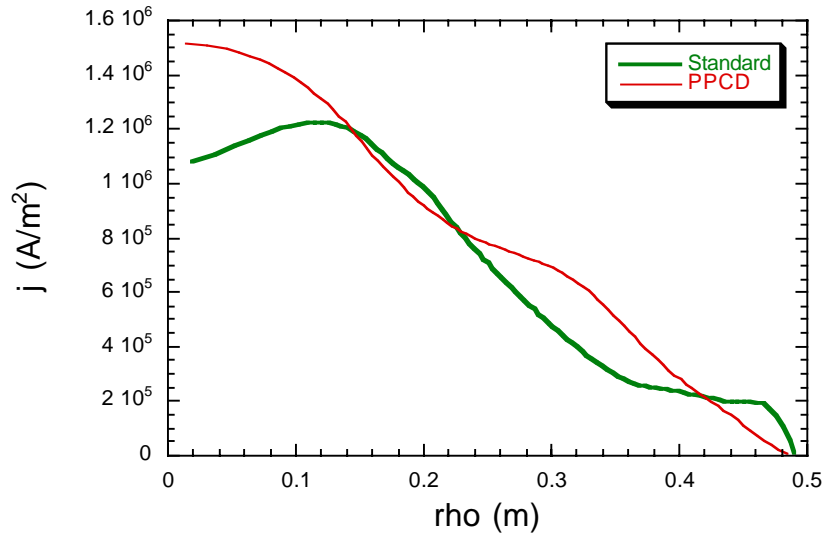
Measured T_e and n_e Profiles



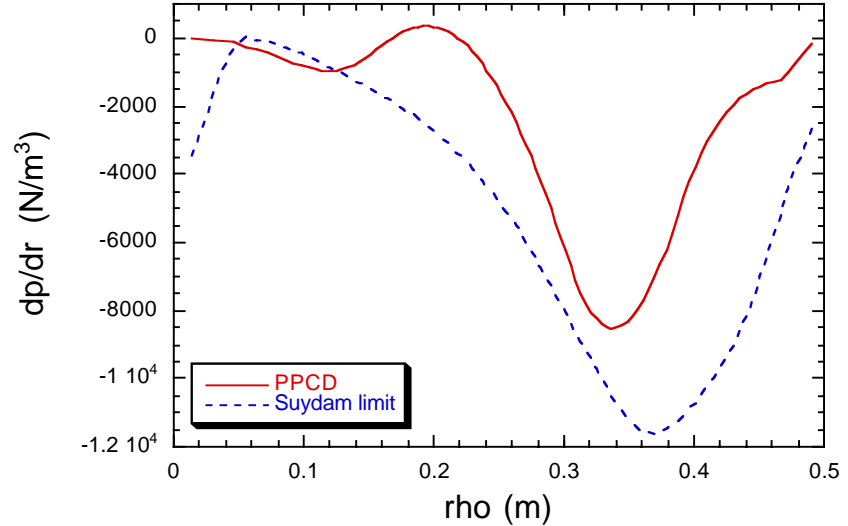
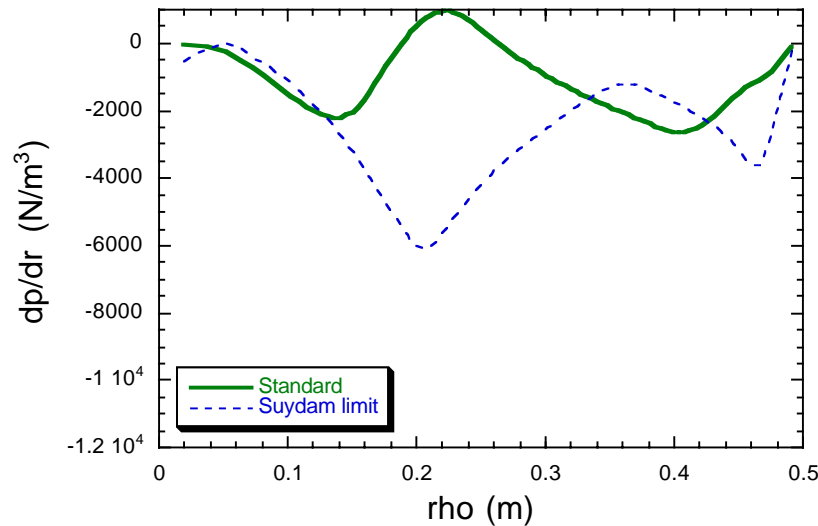
- $T_e(r)$ is measured via 6 radial points of Thomson scattering and via an insertable Langmuir probe at the edge. The combined data is fit to a cubic spline.
- Majority $T_i(\sim 0)$ is measured with Rutherford scattering, and the profile is estimated as $T_i(r)=0.75*T_e(r)$.
- Impurity T_z is measured for C_V using Ion Doppler Spectrometry, and the profile is estimated as $T_z(r)=0.5*T_e(r)$.
- $n_e(r)$ is measured with an 11 chord Far InfraRed Interferometer and Abel inverted using the MSTFIT code.
- Experimental evidence suggests $Z_{\text{eff}} \sim 2$ in the MST. With this approximation and the assumption that C_V is the dominant impurity everywhere, then charge balance determines $n_i(r)$ and $n_z(r)$ from $n_e(r)$:

$$en_i + Zen_z - en_e = 0 \quad Z_{\text{eff}} \equiv \frac{\sum Z_j^2 n_j}{n_e} = \frac{n_i + Z^2 n_z}{n_e}$$

MSTFIT Reconstructed Equilibrium

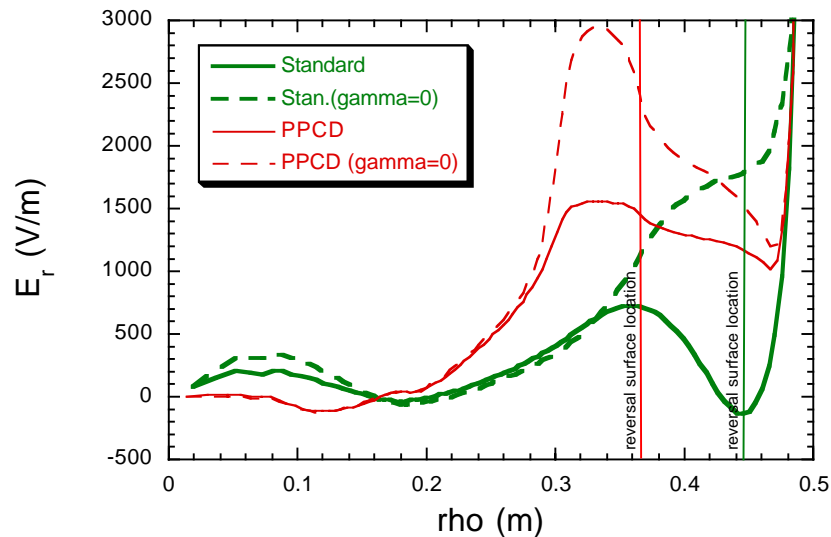
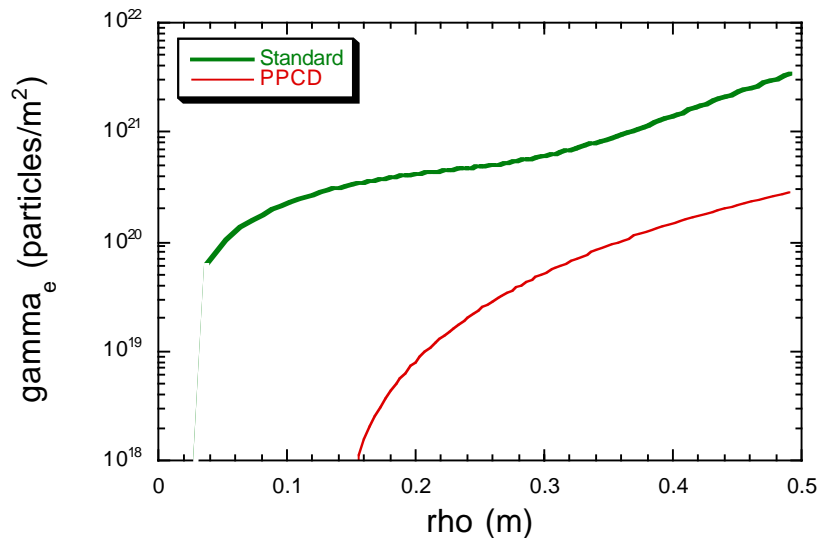


Interchange Mode Stability Limit



- During PPCD the measured pressure gradient drops below the calculated Suydam critical pressure gradient near the edge, meaning that the plasma becomes stable to interchange modes.
- Standard plasmas (and PPCD plasmas at the core) are at the limit of stability to these modes.

Particle Flux and Radial Electric Field

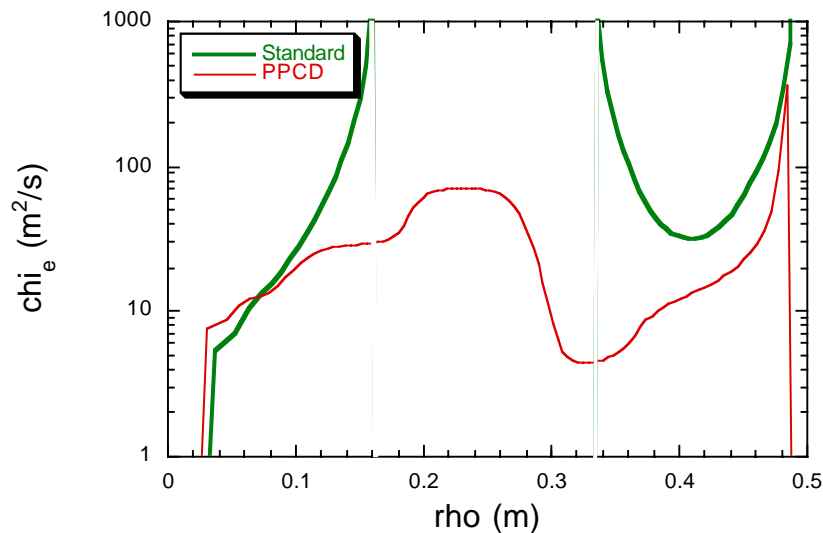
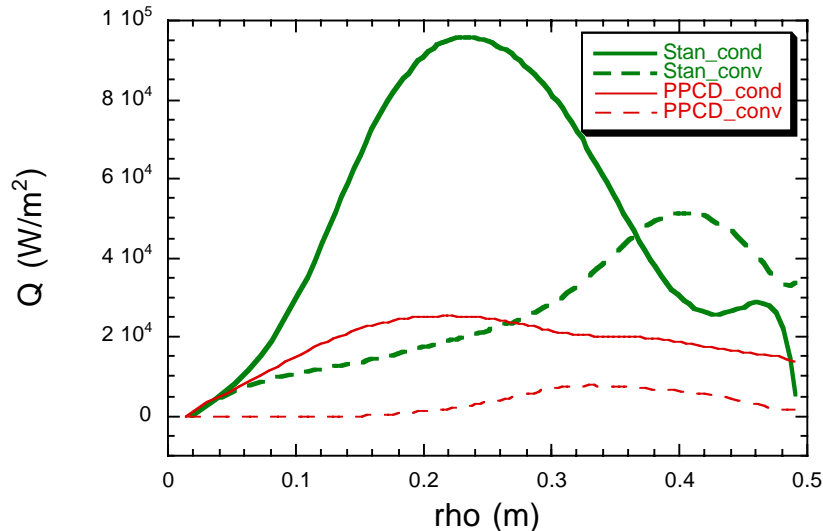


- Particle flux is calculated from an FIR interferometer (n_e) that is co-linear with a D_α array (S_p).
- During PPCD there is a significant reduction in the particle source, which is manifest as a reduction in the particle flux. The core value is unresolvable with this diagnostic setup.
- To first approximation, the ambipolar electric field can be calculated by setting the particle flux to zero. In this case:

$$E_{a,Harvey} \cong -\frac{T_e}{e} \left(\frac{1}{n_e} \frac{\partial n_e}{\partial r} + \frac{1}{2T_e} \frac{\partial T_e}{\partial r} \right)$$
- The deviation from the $\Gamma_e=0$ approximation is important even at low values of flux.

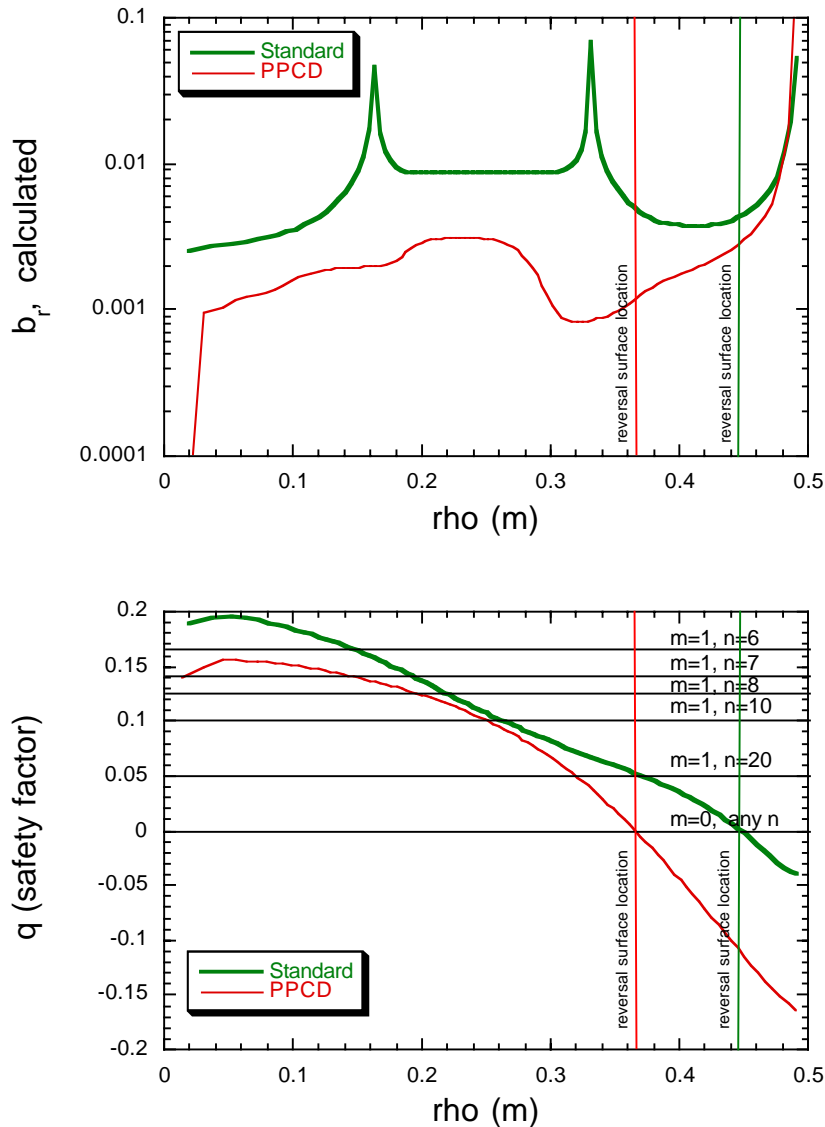
$$\Gamma = -Dn \left(\frac{1}{n} \frac{\partial n}{\partial r} + \frac{1}{2T} \frac{\partial T}{\partial r} - \frac{qE_a}{T} \right)$$

Heat Flux and Thermal Conductivity



- Because the particle flux is largest in the edge of Standard plasmas, it is not surprising to find that heat transport is dominated by convective losses in that region.
- In the region where the dominant magnetic modes of the MST are resonant conductive heat transport is very large.
- Magnetic fluctuations are observed to decrease with the application of PPCD, and we see a corresponding drop in the conductive transport of heat.
- Electron thermal conductivity is consequently improved during PPCD, dropping by roughly a factor of 5 over the bulk of the plasma radius.

Expected Magnetic Fluctuation Level



- If the thermal conductivity has a Rechester-Rosenbluth type form, we can calculate a profile of the expected magnetic fluctuation level:

$$\chi = 2D = \frac{2}{\sqrt{\pi}} v_t D_m \quad D_m = L_{\text{eff}} b_r^2$$

$$L_{\text{eff}}^{-1} = L_{\text{par}}^{-1} + \lambda_{\text{mfp}}^{-1}$$

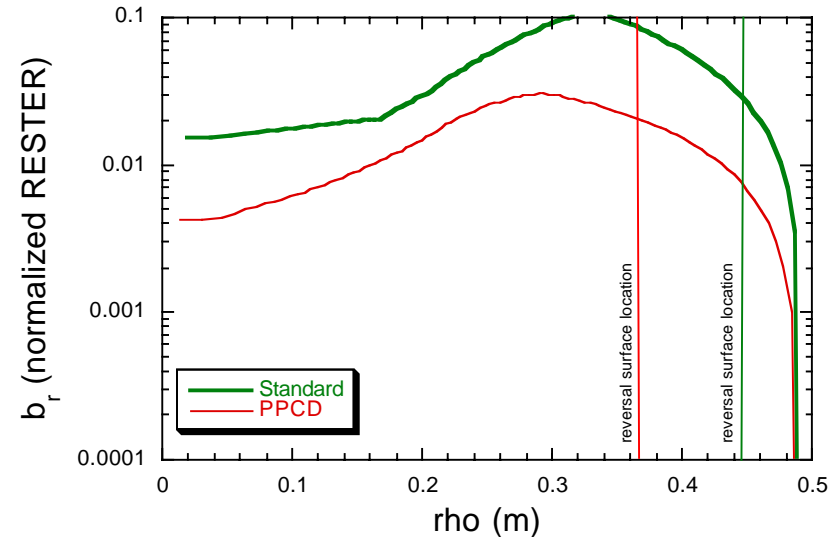
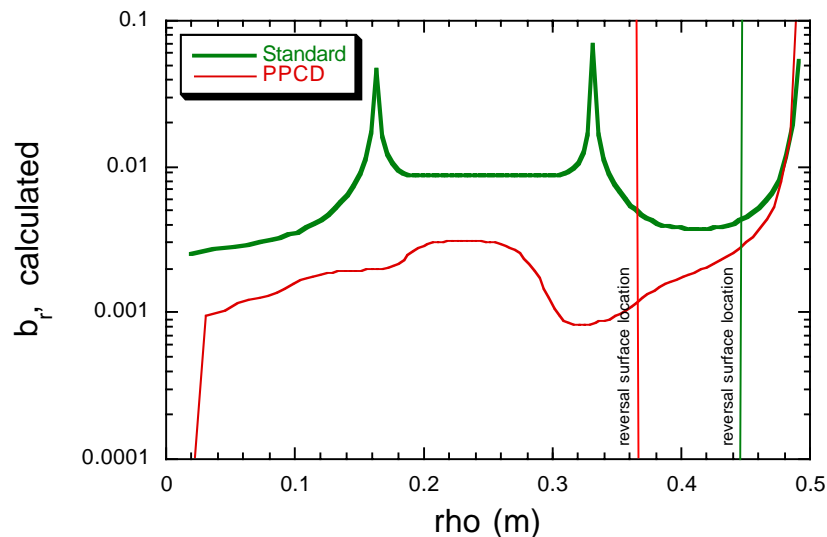
$$L_{\text{par}} \approx a \quad \lambda_{\text{mfp}} \gg a$$

$$D_m \approx a b_r^2$$

$$\chi \approx \frac{2}{\sqrt{\pi}} \sqrt{\frac{2T}{m}} a b_r^2$$

- It is experimentally observed that the magnitude of magnetic fluctuations (as measured at the edge with pick-up coils) drops during PPCD, which is consistent with this calculation, especially in the region of $0.15 < \rho < 0.35$ where the largest MST modes ($n=6,7,8$) are expected to be resonant.

Expected Magnetic Fluctuation Level (continued)



- RESTER calculated linear eigenfunctions for b_r ($m=1$, $n=1-14$) are normalized via the measured B_r gradient (divB=0 enforced pickup coils) at the edge and summed to produce the profile on the right.
- Though the results differ by an order of magnitude, the general trends (rising inboard of the B_T reversal surface, then falling towards the core) are similar.

Conclusions

- Improved particle confinement in the edge of MST (transport barrier?) during PPCD results in reduced overall particle flux and reduced convective heat transport.
- More evidence has been presented that reinforces the notion that heat transport in the MST is driven by magnetic fluctuations.
- Reducing magnetic fluctuations through the application of PPCD results in the reduction of both convective but primarily conductive heat transport and a consequent increase in the overall electron temperature.
- The resultant pressure profile is skirting the calculated Suydam-critical limit, and suggests that residual transport in the MST during PPCD may be due to Interchange and G modes.

Reprints

Full color version of this poster is available online at:

<http://sprott.physics.wisc.edu/biewer/aps2000poster.pdf>
